NANO LETTERS

2006
Vol. 6, No. 12
2718−2722

Shrinking a Carbon Nanotube

T. D. Yuzvinsky,[†,‡,§] W. Mickelson,[†,‡] S. Aloni,[†,‡,||] G. E. Begtrup,[†,‡] A. Kis,[†,‡] and A. Zettl*[,†,‡,§]

Department of Physics, University of California at Berkeley, Materials Sciences Division, Lawrence Berkeley National Laboratory, The Molecular Foundry, Materials Sciences Division, Lawrence Berkeley National Laboratory, and Center of Integrated Nanomechanical Systems, Berkeley, California 94720

Received July 19, 2006; Revised Manuscript Received September 26, 2006

ABSTRACT

We report a method to controllably alter the diameter of an individual carbon nanotube. The combination of defect formation via electron irradiation and simultaneous resistive heating and electromigration in vacuum causes the nanotube to continuously transform into a high-quality nanotube of successively smaller diameter, as observed by transmission electron microscopy. The process can be halted at any diameter. Electronic transport measurements performed in situ reveal a striking dependence of conductance on nanotube geometry. As the diameter of the nanotube is reduced to near zero into the carbon chain regime, we observe negative differential resistance.

Carbon nanotubes form the basis for a wide variety of nanoscale devices, including sensors,[1,2] transistors,[3] actuators,[4] and oscillators.[5] The small size and extraordinary physical properties of carbon nanotubes allow these devices to often exceed the performance of conventional counterparts, accessing higher frequencies and obtaining higher sensitivities. The mechanical and electrical characteristics of nanotubes depend strongly on dimension, with important consequences (moment for oscillators, band gap for transistors, etc.). However, current synthesis methods cannot reliably control the nanotube diameter, and thus nanotube device fabrication is an unpredictable process. Of great utility would be the ability to dictate the exact diameter of a nanotube.

We have developed a method to shrink individual nanotubes to any desired diameter. As the nanotube shrinks, we monitor its electrical conductance. A model is presented which accurately predicts the conductance for arbitrary geometry. In the limit of vanishing nanotube diameter, negative differential resistance is observed, as expected for a carbon chain.

The geometrical tailoring process starts with a multiwalled carbon nanotube (CNT) of arbitrary wall number and diameter. First entire shells are successively removed until a CNT with the desired wall number is achieved. Carbon atoms are then selectively removed from the CNT walls, leaving substantial atomic vacancies. A high-temperature anneal/electromigration treatment shrinks and re-forms the CNT into a high-quality tube of smaller diameter. The process can be repeated in a highly controlled fashion, yielding a high-quality CNT of any preselected and precise diameter. The modification is performed in situ in a transmission electron microscope (TEM) which permits high-resolution real-time monitoring of the CNT geometry, as well as simultaneous dc electrical measurements of the shrinking CNT which can be correlated to the CNT geometry. Importantly, throughout the entire shrinking process the electrical contacts to the CNT remain the same and undisturbed, eliminating contact variances (which have plagued virtually all earlier attempts to correlate CNT geometry and conductance).

We prepare the CNT for simultaneous TEM imaging and electronic characterization by employing a two-probe device architecture with an electron transparent membrane. The membrane is prepared by growing 10−20 nm of silicon nitride on a Si/SiO_2 wafer, which is then back-etched to selectively remove the silicon and silicon oxide layers. Arc-grown nanotubes are deposited onto the membrane out of isopropyl alcohol and located by scanning electron microscopy (SEM). Electrical contacts are patterned by electron beam lithography and deposited via electron beam evaporation of 30 nm of gold. The device is then loaded into a JEOL 2010 TEM with in situ transport capability operating at 100 keV. A Keithley 2410 SourceMeter is used to apply voltages and measure resistance across the two-terminal CNT devices.

Figure 1 shows TEM micrographs of the time evolution of the nanotube device. The initial CNT as shown in Figure 1a has four walls and an outer diameter of 21.5 nm. An applied voltage to the nanotube causes the outer two walls to fail, an effect that has been observed both in vacuum[6−8] and under ambient conditions.[9]

* Corresponding author: azettl@berkeley.edu.
† Department of Physics, University of California at Berkeley.
‡ Materials Sciences Division, Lawrence Berkeley National Laboratory.
§ Center of Integrated Nanomechanical Systems.
|| The Molecular Foundry, Materials Sciences Division, Lawrence Berkeley National Laboratory.

10.1021/nl061671j CCC: $33.50
Published on Web 11/02/2006

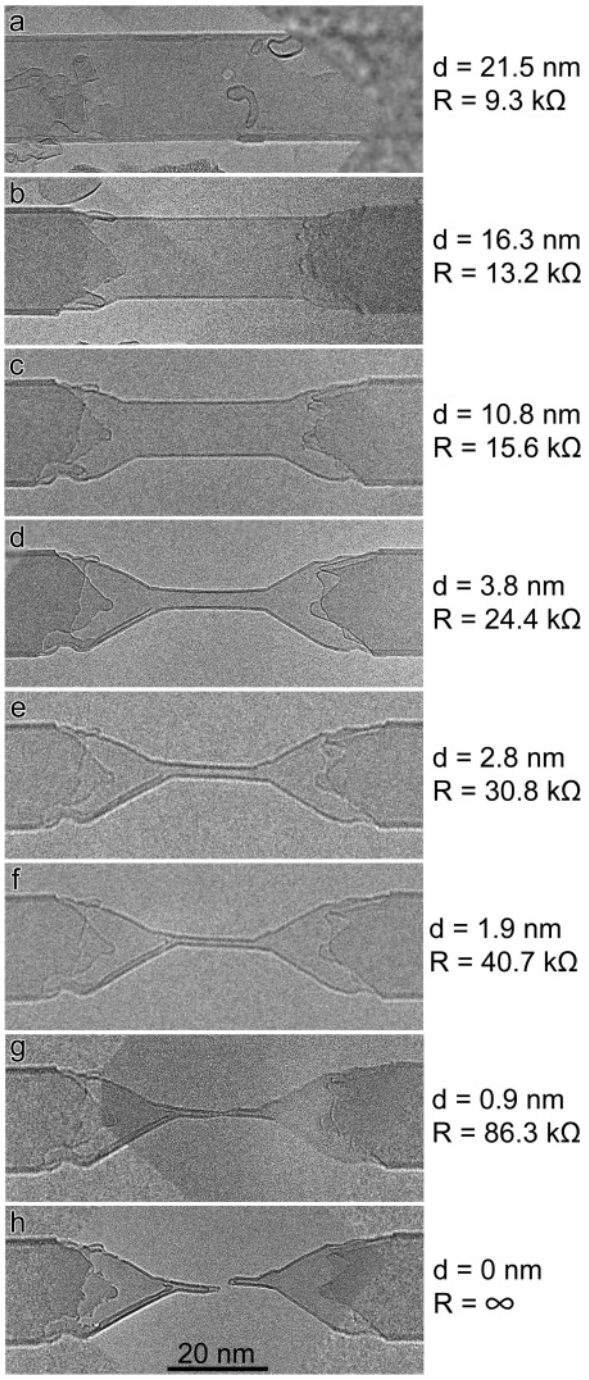

Figure 1. Transmission electron micrographs of a CNT device as it evolves under transport current bias and exposure to the TEM beam. Reducing the applied bias can halt the shrinking process at any time. The minimum CNT diameter and high-bias resistance associated with each image are shown to the right.

To shrink the (in this case two-walled) CNT we more selectively remove carbon atoms from the remaining CNT walls by exploiting knock-on damage induced by the 100 keV TEM electron beam. Such atomic displacement causes numerous vacancy and other defects and a general loss of the perfect nanotube wall graphitic structure,[10−13] and the displaced carbon atoms either are ejected outright or are migrated along the tube.[13] Since we are here most interested in the properties of a high-quality CNT, we require a method to re-form the (fewer) remaining "tube" carbon atoms into

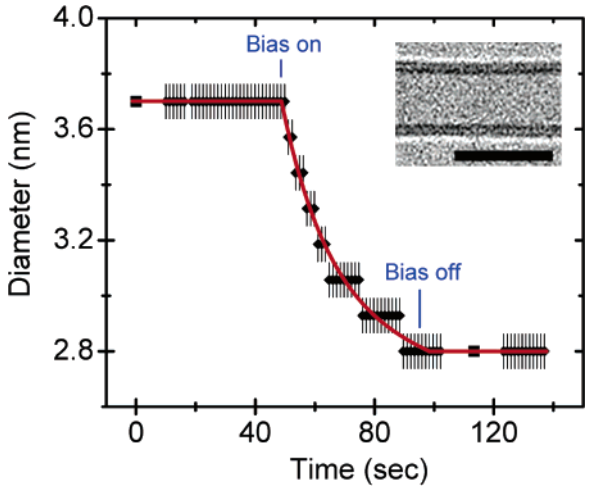

Figure 2. Diameter control of the CNT. Raising (or lowering) the applied bias initiates (or halts) the re-forming process. The two square points are obtained from high-resolution TEM still images, while the remaining data are binned by discrete numbers of pixels obtained from a low-resolution video recording. The curved red line is the sum of two exponentially decaying terms (see text). Inset: A digitally magnified TEM image of the center section of the CNT. The scale bar is 5 nm.

a near-perfect graphitic CNT. This is achieved by the simultaneous application of an electrical current through the CNT device via the electrical contacts, which has two main effects. First, via Joule heating, it increases the temperature of the entire nanotube, allowing for thermal annealing of structural damage.[32] Second, via electromigration of carbon ions, it affords a more rapid reshaping into a defect-free tube (sourcing limited carbon ions where they are needed and sinking them where they are not). The reduced-diameter CNT remains structurally and electrically connected to the original contacts via strain-energy-minimized cones. As shown in the sequentially acquired frames of panels b−f of Figure 1 and in the inset of Figure 2, the shrinking CNT remains clean and retains its distinct, parallel two-wall structure throughout the process. These features distinguish the high quality of the CNT, especially when compared to TEM images of inferior CNTs, which may show surface contamination, corrugations, discontinuities, or interwall defects.[14]

Two competing factors influence how much current should be applied to the nanotube during the shrinking process. First, the applied current must not exceed the threshold for electrical breakdown of the CNT after the desired number of walls has been reached. For arc-grown CNTs, we observe the onset of electrical breakdown at applied voltages in the range 2−3 V. Second, if maximal shrinkage of the nanotube is to occur, the current must be kept as high as possible so as to keep the largest possible length of nanotube at temperatures high enough to anneal out beam damage (comparison with previous studies shows that the maximum CNT temperature is at least 1200 K[7]). In practice, the applied voltage is incrementally increased above 2 V until shrinkage is observed, with the ultimate threshold dependent upon the selected intensity and acceleration voltage of the electron

beam. Once the shrinking process begins, the applied voltage must be tuned to compensate for the changing resistance of the CNT.

We consider briefly the dynamics of the shrinking process. The susceptibility to radiation damage of an atomic lattice can be characterized by the threshold displacement energy E_{thr}, the minimum kinetic energy transfer which can permanently displace an atom from its lattice site. While studies of multiwalled CNTs at room temperature report values of E_{thr} in the range of 15−20 eV,[15] we expect E_{thr} of the shrinking CNT to be much smaller, since in this high temperature regime CNTs become superplastic and can easily be deformed.[32]

We determine E_{thr} by measuring the atomic displacement rate p. A comparison of the 15 nm center region in panels b and f of Figure 1 indicates a loss of ~88% of the carbon atoms, corresponding to an exponential decay with time constant $1/p \approx 1000$ s. The displacement cross section (for simplicity assumed to be isotropic) is given by $\sigma = p/j$, and for a beam current density $j \approx 1$ A/cm^2, we obtain $\sigma \approx 160$ barns. Using the analytical approximation in ref 15 which relates σ to E_{thr}, we estimate the threshold displacement energy under these conditions to be ~5.5 eV, a much smaller value which approaches the E_{thr} of amorphous carbon at room temperature.[15]

As an example of the detailed diameter control of the CNT during the shrinking process, we show in Figure 2 the time evolution of the CNT between two diameter "set points". The initial diameter (equal to 3.7 nm as targeted from an earlier shrinking process) is stable until the current bias is applied. The diameter then decreases smoothly until the new set point of 2.8 nm is reached, whereupon the bias is immediately switched off and the new diameter is locked in. The two square points on the flat parts of the curve in Figure 2 are obtained from high-resolution TEM still images, while the remaining diamond data are obtained from lower resolution video recordings (the discreteness of these data is artificial and due to the inevitable binning of discrete numbers of pixels in the video recording analysis). The curved red line in Figure 2 is a sum of two exponentially decaying terms, with respective time constants 16 and 1000 s. The faster initial re-forming rate (16 s) is due to an increased initial defect density from prior exposure to the TEM beam without an applied bias high enough to initiate re-forming. The slower rate (1000 s) matches the calculated rate for the entire process and is limited by beam-induced defect formation.

The inset to Figure 2 is a TEM image of the tube during the shrinking process, and the well-formed wall images attest to a high tube quality. At a given diameter, blanking of the TEM beam prevents further defects, while continued exposure to the high-energy electrons can be used to increase the number of CNT defects in accordance with the model described above. Thus, our tailoring process allows us not only to select precisely the ultimate diameter of the CNT but also to tune its defect density.

Of prime interest is the connection between the precise CNT geometry and the corresponding electrical conductance.

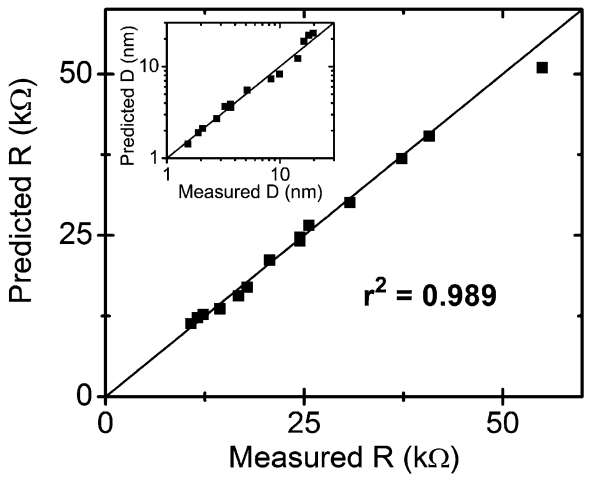

Figure 3. Calculated resistance vs measured resistance of the CNT. The coefficient of determination of the fit is 0.989, increasing to 0.995 if the last point is excluded. Inset: Using the same model we are able to predict the diameter of the smallest section of the nanotube. Logarithmic scales are used to more clearly display the small diameter data.

Previous studies of electronic conduction in CNTs have reported widely varying results, with proposed mechanisms including single ballistic channel conduction, multiple ballistic channel conduction, and fully diffusive transport.[16−18] For multiwalled CNTs the situation is particularly complex, with intertube conduction entering the mix. In particular, the geometrical distribution of high bias current in a multiwalled CNT is in question: reports range from equal amounts of current in each shell[19] to current constrained to the outer shells[16,20] to current distributed uniformly across the entire cross section.[7] Much of this controversy may stem from the different electrical contacts used in each experiment, as even contacts formed by similar macroscopic processes may vary greatly on the nanoscale. The present study circumvents this problem, as the transport properties of CNTs with many different diameters are investigated while keeping the contacts essentially identical.

As the nanotube shrinks, its resistance increases, as shown by the resistance values displayed on the right column of Figure 1. From the chiral dependence of conduction in single-walled carbon nanotubes,[21] one might expect discrete changes in conductance as one wall or the other becomes semiconducting or metallic. We do not observe this. In fact, as our analysis shows, the CNT resistance, irrespective of nanotube diameter, can be accounted for by a simple model that assumes strictly diffusive transport. Figure 3 shows an excellent fit between measured resistance values and resistance values calculated from the geometric model (see Supporting Information for a detailed discussion of model parameters and fitting procedures). We find that the total CNT resistance is dictated wholly by its geometry, with CNT conductance linearly proportional to its cross sectional area.

If the thinning process is allowed to continue, the nanotube eventually fails. As the diameter shrinks below 1 nm, the inner wall finally breaks and endcaps form on both ends, leaving a very thin bridge connecting the two sections of nanotube. This bridge is not stable under the electron beam

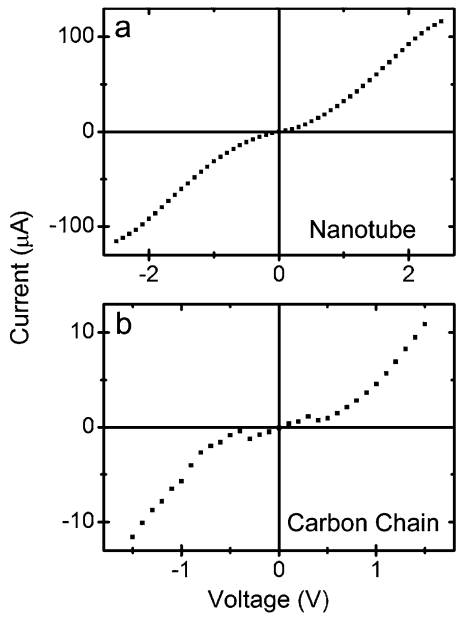

Figure 4. Current−voltage characteristics of the nanotube device. Part a shows a typical characteristic for an intact CNT. Part b shows the characteristic just before failure, in the carbon-chain regime. Negative differential resistance is clearly observed at ±0.3 V.

and rapidly fluctuates, changing appearance from one acquired image to the next. In one instance (shown in Figure 1g) the bridge appears to be a single-walled nanotube (an inner hollow is visible), though in images taken before and after it appears amorphous and the thinnest section cannot be resolved. It is likely that in this regime the bridge assumes a carbon-chain-like structure. In the atomically segmented bridge regime the geometric-based multiwalled CNT conduction model described above obviously breaks down.

Theoretical studies of atomic carbon chains can be used predict the behavior of a bridged (carbon-chain-like) nanotube junction. A key prediction is that of negative differential resistance (NDR) at applied voltages of a fraction of a volt.[22,23] NDR is the basis for a number of semiconductor devices, and the use of components that exhibit NDR can significantly simplify the design of circuits with complicated functions.[24] In recent years, NDR has been observed in a variety of molecular electronics.[25,26,33]

Figure 4 shows transport current−voltage ($I-V$) behavior for our CNT device in two different regimes. Figure 4a corresponds to the device with an intact CNT spanning the contacts, while Figure 4b is in the bridge regime where the nanotube is just failing (between panels g and h in Figure 1). In the bridge regime, the device exhibits NDR at both positive and negative bias of 0.3 V, in agreement with theoretical predictions for atomic carbon chains.

Continued exposure to the electron beam causes any carbon chain bridge to ultimately and permanently fail, and the device becomes electrically insulating, as for Figure 1h. The closed end caps on both the inner and outer wall of the two nanotube segments are clearly visible. It is interesting to note that even after failure, such membrane-anchored devices could serve as templates for single molecule electronics, with the remaining nanotube sections acting as very closely spaced electrodes.[27]

Acknowledgment. The authors thank Adam Fennimore and Steven Konsek for assistance in the early stages of this project, and Kenny Jensen for MATLAB assistance. This work was supported in part by the Director, Office of Energy Research, Office of Basic Energy Sciences, Materials Sciences Division of the US Department of Energy under Contract No. DE-AC-03-76SF00098 and by the National Science Foundation under Grant No. EEC-0425914, supporting the Center of Integrated Nanomechanical Systems.

Supporting Information Available: A detailed discussion of geometric model parameters and fitting procedures and animation of nanotube shrinking. This material is available free of charge via the Internet at http://pubs.acs.org.

References

(1) Collins, P. G.; Bradley, K.; Ishigami, M.; Zettl, A. *Science* **2000**, *287*, 1801.
(2) Kong, J.; Franklin, N. R.; Zhou, C.; Chapline, M. G.; Peng, S.; Cho, K.; Dai, H. *Science* **2000**, *287*, 622.
(3) Tans, S. J.; Verschueren, A. R. M.; Dekker, C. *Nature* **1998**, *393*, 49.
(4) Fennimore, A. M.; Yuzvinsky, T. D.; Han, W. Q.; Fuhrer, M. S.; Cumings, J.; Zettl, A. *Nature* **2003**, *424*, 408.
(5) Papadakis, S. J.; Hall, A. R.; Williams, P. A.; Vicci, L.; Falvo, M. R.; Superfine, R.; Washburn, S. *Phys. Rev. Lett.* **2004**, *93*, 146101.
(6) Cumings, J.; Collins, P. G.; Zettl, A. *Nature* **2000**, *406*, 586.
(7) Yuzvinsky, T. D.; Mickelson, W.; Aloni, S.; Konsek, S. L.; Fennimore, A. M.; Begtrup, G. E.; Kis, A.; Regan, B. C.; Zettl, A. *Appl. Phys. Lett.* **2005**, *87*, 083103.
(8) Huang, J. Y.; Chen, S.; Jo, S. H.; Wang, Z.; Han, D. X.; Chen, G.; Dresselhaus, M. S.; Ren, Z. F. *Phys. Rev. Lett.* **2005**, *94*, 236802.
(9) Collins, P. G.; Arnold, M. S.; Avouris, P. *Science* **2001**, *292*, 706.
(10) Ajayan, P. M.; Ravikumar, V.; Charlier, J.-C. *Phys. Rev. Lett.* **1998**, *81*, 1437.
(11) Chopra, N. G.; Ross, F. M.; Zettl, A. *Chem. Phys. Lett.* **1996**, *256*, 241.
(12) Crespi, V. H.; Chopra, N. G.; Cohen, M. L.; Zettl, A.; Louie, S. G. *Phys. Rev. B* **1996**, *54*, 5927.
(13) Banhart, F.; Li, J. X.; Krasheninnikov, A. V. *Phys. Rev. B* **2005**, *71*, 241408(R) .
(14) Molhave, K.; Gudnason, S. B.; Pedersen, A. T.; Clausen, C. H.; Horsewell, A.; Boggild, P. *Nano Lett.* **2006**, *6*, 1663.
(15) Banhart, F. *Rep. Prog. Phys.* **1999**, *62*, 1181.
(16) Frank, S.; Poncharal, P.; Wang, Z. L.; de Heer, W. A. *Science* **1998**, *280*, 1744.
(17) Li, H. J.; Lu, W. G.; Li, J. J.; Bai, X. D.; Gu, C. Z. *Phys. Rev. Lett.* **2005**, *95*, 086601.
(18) Langer, L.; Bayot, V.; Grivei, E.; Issi, J.-P.; Heremans, J. P.; Olk, C. H.; Stockman, L.; Van Haesendonck, C.; Bruynseraede, Y. *Phys. Rev. Lett.* **1996**, *76*, 479.
(19) Collins, P. G.; Hersam, M.; Arnold, M.; Martel, R.; Avouris, P. *Phys. Rev. Lett.* **2001**, *86*, 3128.
(20) Bourlon, B.; Miko, C.; Forro, L.; Glattli, D. C.; Bachtold, A. *Phys. Rev. Lett.* **2004**, *93*.
(21) Saito, R.; Dresselhaus, G.; Dresselhaus, M. S. *Physical Properties of Carbon Nanotubes*; World Scientific Publishing Company: Singapore, 1998.
(22) Larade, B.; Taylor, J.; Mehrez, H.; Guo, H. *Phys. Rev. B* **2001**, *64*, 075420.
(23) Neaton, J. B.; Khoo, K. H.; Spataru, C. D.; Louie, S. G. *Comput. Phys. Commun.* **2005**, *169*, 1.
(24) Chen, J.; Wang, W.; Klemic, J.; Reed, M. A.; Axelrod, B. W.; Kaschak, D. M.; Rawlett, A. M.; Price, D. W.; Dirk, S. M.; Tour, J. M.; Grubisha, D. S.; Bennett, D. W. *Ann. N. Y. Acad. Sci.* **2002**, *960*, 69.
(25) Chen, J.; Reed, M. A.; Rawlett, A. M.; Tour, J. M. *Science* **1999**, *286*, 1550.
(26) Gaudioso, J.; Lauhon, L. J.; Ho, W. *Phys. Rev. Lett.* **2000**, *85*, 1918.

(27) Zandbergen, H. W.; van Duuren, R. J. H. A.; Alkemade, P. F. A.; Lientschnig, G.; Vasquez, O.; Dekker, C.; Tichelaar, F. D. *Nano Lett.* **2005**, *5*, 549.
(28) Romano, J. D.; Price, R. H. *Am. J. Phys.* **1996**, *64*, 1150.
(29) Petrov, V. A.; Petrova, I. I.; Chekhovskoi, V. Y.; Sheindlin, A. E. *High Temp.−High Pressures* **1970**, *2*, 161.
(30) Klein, C. A. *Rev. Mod. Phys.* **1962**, *34*, 56.
(31) Kinchin, G. H. *Proc. R. Soc. London* **1953**, *A217*, 9.
(32) Huang, J. Y.; Chen, S.; Wang, Z. Q.; Kempa, K.; Wang, Y. M.; Jo, S. H.; Chen, G.; Dresselhaus, M. S.; Ren, Z. F. *Nature* **2006**, *439*, 281.
(33) Pop, E.; Mann, D.; Cao, J.; Wang, Q.; Goodson, K.; Dai, H. *Phys. Rev. Lett.* **2005**, *95*, 155505.

NL061671J